PHOTONICS Research

One-step implementation of Rydberg-antiblockade SWAP and controlled-SWAP gates with modified robustness

Jin-Lei Wu,[1] Yan Wang,[1] Jin-Xuan Han,[1] Yu-Kun Feng,[1] Shi-Lei Su,[2] Yan Xia,[3] Yongyuan Jiang,[1] and Jie Song[1,*]

[1]School of Physics, Harbin Institute of Technology, Harbin 150001, China
[2]School of Physics and Microelectronics, Zhengzhou University, Zhengzhou 450001, China
[3]Department of Physics, Fuzhou University, Fuzhou 350002, China
*Corresponding author: jsong@hit.edu.cn

Received 24 November 2020; revised 2 March 2021; accepted 7 March 2021; posted 8 March 2021 (Doc. ID 415795); published 29 April 2021

The prevalent fashion of executing Rydberg-mediated two- and multi-qubit quantum gates in neutral atomic systems is to pump Rydberg excitations using multistep piecewise pulses in the Rydberg blockade regime. Here, we propose to synthesize a Λ-type Rydberg antiblockade (RAB) of two neutral atoms using periodic fields, which facilitates one-step implementations of SWAP and controlled-SWAP (CSWAP) gates with the same gate time. Besides, the RAB condition is modified so as to circumvent the sensitivity of RAB-based gates to infidelity factors, including atomic decay, motional dephasing, and interatomic distance deviation. Our work makes up the absence of one-step schemes of Rydberg-mediated SWAP and CSWAP gates and may pave a way to enhance the robustness of RAB-based gates.

https://doi.org/10.1364/PRJ.415795

1. INTRODUCTION

The interaction between neutral atoms excited to Rydberg states is strong and long-range, making Rydberg atoms attractive in the context of quantum technologies [1–4]. Rydberg atoms have been considered as an attractive candidate platform for quantum computing [5–7] and quantum simulating [8–10] because of remarkable and continuous advances in cooling, trapping, and manipulating neutral atoms. Entangled states with scale up to 20 qubits have been generated in arrays of Rydberg atoms [11]. Furthermore, atomic species in experiments have been generalized from alkali metal atoms to alkaline earth atoms [12]. Although various schemes have been put forward to implement Rydberg-mediated quantum gates since the pioneering protocol was reported [13], enormous challenges remain in achieving experimentally high-fidelity Rydberg gates as well as in highly efficient Rydberg-atom-based quantum computing [1–4]. On the one hand, the gate fidelity is always limited due to intrinsic and technical errors. Intrinsic errors involve atomic decay and imperfect approximate conditions, including blockade errors in the Rydberg blockade [1,14–16] gate schemes [13,17–20], nonadiabatic errors [21,22] in adiabatic gate schemes [13,23–27], and higher-order perturbation errors in Rydberg antiblockade (RAB) [28–33] gate schemes [34–40]. Technical errors are caused by imperfections of techniques in, e.g., cooling, trapping, and manipulating atoms [1,2,41,42]. On the other hand, existing schemes are not sufficient for one-step implementing certain two-qubit gates and many multi-qubit gates, especially for some frequently used gates, such as the SWAP gate, and the controlled-SWAP (CSWAP), that is, the Fredkin gate [43].

Despite a controlled-not (CNOT) gate combined with a small number of single-qubit gates constructing arbitrary gate operations (e.g., a SWAP gate formed with three CNOT gates [44]), direct executions of quantum gates can significantly improve the processing efficiency of lengthy quantum algorithms rather than decomposing them into a series of elementary gates [25,45–48]. The SWAP gate is an important, nontrivial two-qubit gate with extensive applications in quantum computation [49], entanglement swapping [50], and quantum repeaters [51]. The CSWAP gate is one of the most representative multi-qubit gates, swapping the quantum states of two target qubits depending on the state of a control qubit, which holds important functions in quantum error correction [52], quantum fingerprinting [53], and quantum routers [54]. Among existing Rydberg-mediated gate schemes, SWAP gates are achieved in three or more steps, using multiple piecewise pulses and involving two or more Rydberg states in single atoms [55–57]. The scheme of implementing a CSWAP gate requires five-step operations with five piecewise pulses [58]. The multi-step operations of implementing quantum gates not only make

quantum algorithms rigmarole and unproductive but also accumulate more decoherence.

In the present work, we propose schemes to implement one-step SWAP and CSWAP gates of Rydberg atoms that are driven by periodic amplitude-modulated (AM) fields. The synthetic interplay between AM fields and interatomic Rydberg–Rydberg interaction (RRI) induces a Λ-type RAB structure of two atoms, based on which a SWAP gate on two atoms and a CSWAP gate on three atoms can be formed. However, similar to existing RAB-based gate schemes [34–37,59,60], the attendance of a doubly excited Rydberg state $|rr\rangle$ during the evolution will induce common issues in RAB-based gates, i.e., the sensitivity to atomic decay, motional dephasing, and interatomic distance deviation. Aiming at these common issues, we modify the RAB condition to constrain the participation of $|rr\rangle$ in the gate procedure, which can not only reduce the effect of atomic decay from Rydberg states and of motional dephasing during Rydberg excitation but also loosen the stringent restrictions on the parameter condition of RAB to a certain degree. The present work fills the gap of directly constructing Rydberg-atom SWAP and CSWAP gates in one step. In addition, the work may also pave the way to circumvent the common issues in RAB-based gates.

This paper is organized as follows. In Section 2, we illustrate the construction of a Λ-type RAB structure, based on which one-step SWAP gates are implemented with resonant and modified RAB, respectively. In Section 3, the robustness of two kinds of SWAP gates is studied and compared. In Section 4, we propose to implement a CSWAP gate in one step. A conclusion is given in Section 5.

2. SWAP GATES BASED ON RYDBERG ANTIBLOCKADE

A. Resonant Λ-Type Rydberg Antiblockade

As shown in Fig. 1(a), the interaction of the laser-driven two atoms is described by the Hamiltonian ($\hbar = 1$)

$$\hat{H}_{12} = \hat{H}_1 \otimes \hat{\mathcal{I}}_2 + \hat{\mathcal{I}}_1 \otimes \hat{H}_2 + V|rr\rangle\langle rr|, \tag{1}$$

where $V|rr\rangle\langle rr|$ with $|rr\rangle \equiv |r\rangle_1 \otimes |r\rangle_2$ denotes the two-atom RRI, and $\hat{\mathcal{I}}_j$ $(j = 1, 2)$ is the identity operator of the jth atom. $\hat{H}_j$, the individual Hamiltonian of the jth laser-driven atom, reads

$$\hat{H}_j = \sum_{k=0}^{1} \frac{\Omega_k(t)}{2} |k\rangle_j\langle r| + \text{H.c.} \tag{2}$$

We impose resonant AM laser fields on the two atoms to induce AM Rabi frequencies $\Omega_k(t) = \Omega_{km} \cos(\omega_k t)$ $(k = 0, 1)$, where Ω_{km} is the maximum and ω_k the modulation frequency. We separate V into $V = \delta + \delta_0$, where we define $\delta \equiv \omega_1 - \omega_0$ whose function is to compensate for the detuning of the transition $|01\rangle(|10\rangle) \leftrightarrow |rr\rangle$ so as to induce the RAB, while δ_0 is a small quantity with $\delta \gg \delta_0$ whose function is to neutralize the Stark shift of $|rr\rangle$ cased by the AM fields. When considering the parameter condition $|\omega_0|, |\omega_1|, |\omega_0 - \delta|, |\omega_1 + \delta| \gg |\Omega_{0m}|/4$, $|\Omega_{1m}|/4$, with the second-order perturbation theory [61,62] the two-atom Hamiltonian can be reduced toward an effective form (see Appendix A):

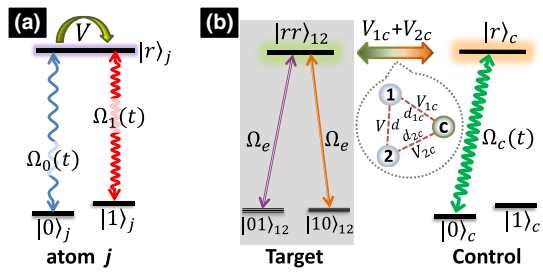

Fig. 1. (a) Schematic for implementing a SWAP gate. Two identical atoms are driven resonantly by two AM laser fields, excited from two ground (computational) states $|0\rangle$ and $|1\rangle$ to a Rydberg (mediated) state $|r\rangle$, respectively, with modulated Rabi frequencies $\Omega_0(t)$ and $\Omega_1(t)$. Two atoms are coupled to each other by RRI with strength $V = C_6/d^6$, C_6 being the van der Waals coefficient and d the interatomic distance. The effective Λ-type RAB dynamics is shown in the shadow of (b). (b) Schematic for implementing a CSWAP gate. Inset circle: the control atom c is coupled to target atoms 1 and 2 described in (a), with RRI strengths V_{1c} and V_{2c} corresponding to interatomic distances d_{1c} and d_{2c}, respectively. The effective Λ-type system of the target atoms is coupled to the control atom with RRI strength $(V_{1c} + V_{2c})$. In addition, the control atom is excited resonantly by another AM field from $|0\rangle_c$ to $|r\rangle_c$ with Rabi frequency $\Omega_c(t)$.

$$\hat{H}_e = \left[\frac{\Omega_e}{2}(|01\rangle\langle rr| + |10\rangle\langle rr|) + \text{H.c.}\right] + \delta'|rr\rangle\langle rr|, \tag{3}$$

in which $\Omega_e = \Omega_{0m}\Omega_{1m}/8\omega_1 - \Omega_{0m}\Omega_{1m}/8\omega_0$ is the effective Rabi frequency of the second-order double Rydberg pumping, and $\delta' = \Delta_{rr} + \delta_0$ with $\Delta_{rr} = \Omega_{0m}^2/8\omega_1 - \Omega_{1m}^2/8\omega_0 + \Omega_{1m}^2/8(\omega_1 + \delta) - \Omega_{0m}^2/8(\omega_0 - \delta)$ being the Stark shift of the Rydberg pair state $|rr\rangle$.

The effective quantum system described by Eq. (3) indicates a Λ-type RAB structure where the doubly excited Rydberg pair state $|rr\rangle$ mediates the transition between two odd-parity computational states $|01\rangle$ and $|10\rangle$, while even-parity states $|00\rangle$ and $|11\rangle$ remain unaffected. A SWAP gate can be implemented through a resonant Raman-like process $|01\rangle \leftrightarrow |rr\rangle \leftrightarrow |10\rangle$ with the resonance condition $\delta' = 0$ and gate time $T = \sqrt{2}\pi/|\Omega_e|$; further, the SWAP gate is of the form $U_{\text{SWAP}} = |00\rangle\langle 00| - |01\rangle\langle 10| - |10\rangle\langle 01| + |11\rangle\langle 11|$, which is equivalent to the standard form up to local phase operations.

For identifying the gate validity, we simulate numerically the gate performance by solving the master equation

$$\dot{\rho} = i[\rho, \hat{H}_{\text{Full}}] - \frac{1}{2}\sum_{j=1}^{N}\sum_{k=0}^{2}(\hat{\mathcal{L}}_k^{j\dagger}\hat{\mathcal{L}}_k^j\rho - 2\hat{\mathcal{L}}_k^j\rho\hat{\mathcal{L}}_k^{j\dagger} + \rho\hat{\mathcal{L}}_k^{j\dagger}\hat{\mathcal{L}}_k^j), \tag{4}$$

in which ρ is the density operator and $\dot{\rho}$ the time derivative of the density operator. $\hat{H}_{\text{Full}}$ denotes the full Hamiltonian of the atomic system [for the SWAP gate $\hat{H}_{\text{Full}}$ is Eq. (1)]. $N = 2$ $(N = 3)$ is the number of atoms for the SWAP (CSWAP) gate. The atomic decay operator is defined by $\hat{\mathcal{L}}_k^j \equiv \sqrt{\gamma_k}|k\rangle_j\langle r|$, for which an additional ground state $|2\rangle_j$ is introduced to denote those Zeeman magnetic sublevels out of the computational states $|0\rangle_j$ and $|1\rangle_j$. In this work, we assume that ^{87}Rb atoms are adopted, and decay rates from a Rydberg state into eight Zeeman ground states are identical for convenience, so

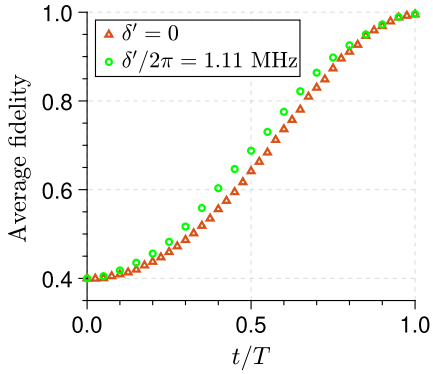

Fig. 2. Time-dependent average fidelities of the SWAP gate with $\{\delta' = 0,\ T = 3.87\ \mu s\}$ and $\{\delta'/2\pi = 1.11$ MHz, $T = 33.28\ \mu s\}$, respectively. Atomic decay is not considered.

$\gamma_0 = \gamma_1 = 1/8\tau$ and $\gamma_2 = 3/4\tau$ with τ being the lifetime of the Rydberg state.

The computational states can be encoded on the hyperfine ground states $|0\rangle = |5S_{1/2}, F = 1, m_F = 0\rangle$ and $|1\rangle = |5S_{1/2}, F = 2, m_F = 0\rangle$. We choose a suitable set of parameters $\Omega_{0m}/2\pi = 5.6$ MHz, $\Omega_{1m}/2\pi = 16.4$ MHz, $\omega_{0m}/2\pi = 40$ MHz, and $\omega_{1m}/2\pi = 110$ MHz, which gives $|\Omega_e|/2\pi = 183.6$ kHz, $T = 3.872\ \mu s$, and $\Delta_{rr}/2\pi = -487.4$ kHz. For $\delta' = 0$, $V/2\pi = 70.49$ MHz can be attained, which is experimentally feasible, for example, with $\{|r\rangle = |70S_{1/2}\rangle$ $(C_6/2\pi = 858.4\ \text{GHz}\cdot\mu\text{m}^6)$, $d \sim 4.8\ \mu m\}$ or $\{|r\rangle = |100S_{1/2}\rangle$ $(C_6/2\pi = 56.2\ \text{THz}\cdot\mu\text{m}^6)$, $d \sim 9.6\ \mu m\}$. To illustrate performance of the SWAP gate, in Fig. 2 we numerically calculate the trace-preserving-quantum-operator-based average fidelity [34,38,63] (see Appendix B for definition). The average fidelity of the SWAP gate with $\delta' = 0$ reaches >0.995.

B. Modified Condition of Rydberg Antiblockade

The SWAP gate noted above is not robust. The Rydberg pair state $|rr\rangle$ attends significantly the gate procedure, which will cause nonignorable decay errors. More notably, the gate is sensitive to fluctuations in RRI strength (interatomic distance) and is susceptible to motion-induced dephasing due to finite atomic temperature, which are common and intractable issues in RAB-based gates [34–37,40,59,60,64,65] such that to experimentally implement them with a high-fidelity suffers from great difficulties. In order to circumvent these issues, reducing participation of $|rr\rangle$ in the gate procedure can be an effective approach [38,66,67], which not only reduces atomic decay errors but also relaxes the demanding RAB condition and weakens effect of motional dephasing. To this end, we consider the large-detuning condition $|\delta'| \gg |\Omega_e|/2$ for the Λ-type RAB structure described by Eq. (3). Then, a modified format of RAB can be obtained, holding an effective ground-state exchange interaction between two atoms, described by

$$\hat{H}_{dd} = -\frac{\Omega_{dd}}{2}(|01\rangle + |10\rangle)(\langle 01| + \langle 10|), \tag{5}$$

with $\Omega_{dd} = \Omega_e^2/2\delta'$. Thus, a SWAP gate U_{SWAP} can be achieved with gate time $T = \pi/|\Omega_{dd}|$. With $\delta'/2\pi = 1.11$ MHz corresponding to $T = 33.28\ \mu s$, the average gate fidelity can also reach >0.995 [see Fig. 2]. The modified condition $|\delta'| \gg |\Omega_e|/2$ of RAB suppresses the excitation of the doubly excited Rydberg state $|rr\rangle$, which can be found in Fig. 3, where we compare the situations of the resonant RAB [Fig. 3(a)] and the modified RAB [Fig. 3(b)] by plotting Rydberg excitation probabilities with different excitation numbers. From Fig. 3, we learn that the single-excitation states are hardly populated for both cases. More importantly, the double-excitation Rydberg pair state $|rr\rangle$ is significantly constrained for the modified RAB, and its excitation probability is less than 0.015 throughout the gate procedure.

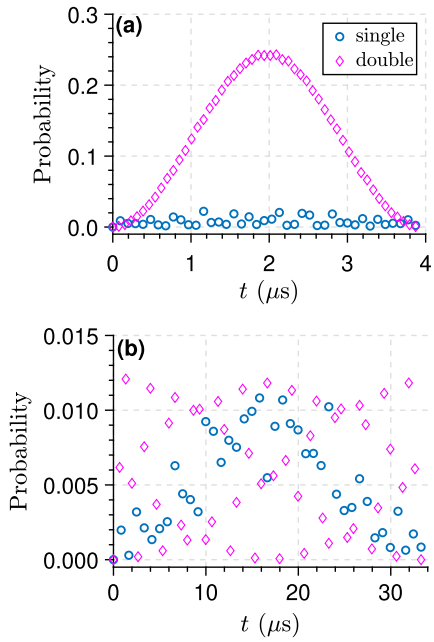

Fig. 3. Rydberg excitation probabilities during the SWAP gate procedure with different excitation numbers for (a) the resonant RAB with $\delta' = 0$ and (b) the modified RAB with $\delta'/2\pi = 1.11$ MHz, respectively. Two-atom initial product state $|\Psi_0\rangle = (|0\rangle_1 + |1\rangle_1)/\sqrt{2} \otimes |1\rangle_2$ is specified.

3. SWAP GATE WITH MODIFIED ROBUSTNESS

For the conventional Rydberg-antiblockade quantum gates, a key property is the participation of the Rydberg pair state $|rr\rangle$ in the gate procedure mediating the state shifts of ground states, so the gate operations on atomic ground states suffer from decay from Rydberg states, laser dephasing caused by atomic motions due to the Doppler effect. Besides, to guarantee the attendance of $|rr\rangle$, the RAB condition with a strict relation among ω_0, ω_1, and V must be precisely controlled, which makes the gate operations sensitive to errors in V. However, for the modified RAB described by the effective Hamiltonian in Eq. (5), $|rr\rangle$ is not needed in the gate procedure, so the issues above will be efficiently evaded.

In the following, we investigate and compare infidelities of the SWAP gates obtained by the resonant RAB and the modified RAB, taking into account atomic decay originated from a finite lifetime of the Rydberg state, motional dephasing due to finite atomic temperature, and fluctuations in RRI strength

caused by interatomic distance deviation. For simplicity, a two-atom initial product state $|\Psi_0\rangle = (|0\rangle_1 + |1\rangle_1)/\sqrt{2} \otimes |1\rangle_2$ is specified, and the gate fidelity is defined by $F \equiv \mathrm{tr}(\rho|\Psi\rangle\langle\Psi|)$ with $|\Psi\rangle = U_{\mathrm{SWAP}}|\Psi_0\rangle$. From Fig. 4(a), we learn that the infidelity of the SWAP gate obtained by the modified RAB is reduced compared with that obtained by the resonant RAB, even though the gate time is prolonged by near 10 multiples. The gate infidelity for the modified RAB can decrease to below 10^{-3} with $\tau > 500$ μs.

Due to the atomic thermal motion, processes of Rydberg excitations suffer from motional dephasing inevitably because of presence of the Doppler effect [2,68,69], which is an important resource of technical errors. When considering motional dephasing, the Rabi frequencies of the Rydberg excitation in Eq. (2) are changed, as $\Omega_k(t) \to \Omega_k(t)e^{i\Delta_k t}$ $(k = 0, 1)$ [42,68,69]. The detunings $\Delta_{0,1}$ of the Rydberg pumping lasers seen by the atoms are two random variables yielded with a Gaussian probability distribution of the mean $\bar{\Delta} = 0$ and the standard deviation $\sigma_\Delta = k_{\mathrm{eff}} v_{\mathrm{rms}}$, where k_{eff} is the effective wave vector magnitude of lasers that atoms undergo, and $v_{\mathrm{rms}} = \sqrt{k_B T_a/M}$ is the atomic root-mean-square velocity with k_B, T_a, and M being the Boltzmann constant, atomic temperature, and atomic mass, respectively. Here, we suppose for simplicity that there are two counterpropagating laser fields with wavelengths $\lambda_1 \sim 480$ nm and $\lambda_2 \sim 780$ nm used for excitation of the Rydberg state $|r\rangle = |100S_{1/2}\rangle$ through a two-photon process with the intermediate state $|p\rangle = |5P_{3/2}\rangle$ [68], which gives an effective wave vector magnitude $k_{\mathrm{eff}} \sim 5 \times 10^6$ m^{-1} [42]. Then, with these settings, we numerically work out in Fig. 4(b) the infidelities of the SWAP gates obtained by the resonant RAB and the modified RAB, respectively. The gate infidelity for the modified RAB is dramatically reduced by even an order of magnitude when $T_a > 30$ μK, compared with that for the resonant RAB. With an experimentally accessible atomic temperature $T_a \sim 10$ μK [5,7], the infidelity caused by motional dephasing can be below 10^{-2}.

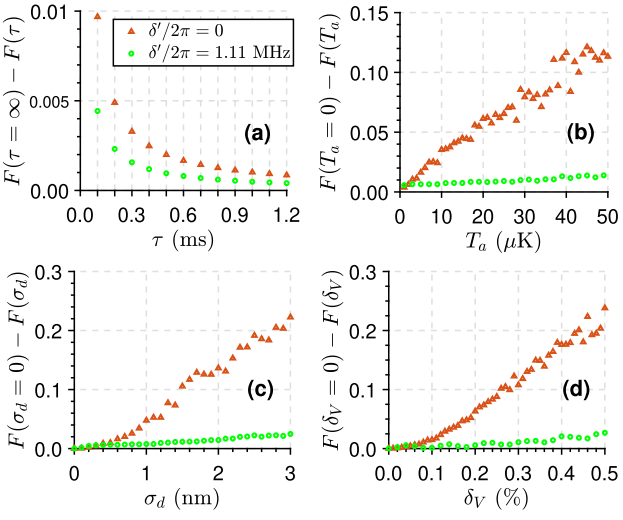

Fig. 4. Infidelities of the SWAP gates caused by (a) atomic decay with different lifetimes of the Rydberg state, (b) motional dephasing with different atomic temperatures, (c) standard deviations of the interatomic distance, and (d) deviations in the RRI strength. Each point in (b), (c), and (d) denotes the average of 201 results.

For controlling the RRI strength between the atoms, interatomic distance cannot be strictly fixed owing to imperfections of cooling and trapping atoms, and it can be characterized with a quasi-1D Gaussian probability distribution of the mean (ideal) $d = \sqrt[6]{C_6/V}$ and the standard deviation σ_d [6]. From Fig. 4(c), we know that, while the gate performance is still sensitive to the interatomic distance deviation, the modified RAB can loosen this sensitivity to a certain degree. More intuitively, we consider a relative deviation δ_V to change the RRI strength into $V[1 + \mathrm{rand}(\delta_V)]$, where $\mathrm{rand}(\delta_V)$ is a function creating random numbers within $[-\delta_V, \delta_V]$. Figure 4(d) shows the effect of different δ_V on the fidelities of implementing the SWAP gates. It is apparent that increasing the relative deviation in V reduces the fidelity of the SWAP gates significantly for the case of the resonant RAB, while the effect of δ_V on the SWAP gate of the modified RAB is much slighter, which indicates that the gate performance against the deviations in V is largely improved by the modified RAB.

4. ONE-STEP IMPLEMENTATION OF CSWAP GATES

Finally, we illustrate one-step implementation of a CSWAP gate, for which a control atom (termed c) is introduced, whose state determines whether or not the SWAP gate on atoms 1 and 2 can be executed. The schematic concerning Rydberg pumping and interatomic RRI is detailed in Fig. 1(b). The interaction of the laser-driven three atoms is described by a full Hamiltonian

$$\hat{H}_{12c} = \hat{H}_{12} \otimes \hat{\mathcal{I}}_c + \hat{\mathcal{I}}_1 \otimes \hat{\mathcal{I}}_2 \otimes \hat{H}_c + \hat{\mathcal{I}}_1 \otimes V_{2c}|rr\rangle_{2c}\langle rr| + V_{1c}|r\rangle_1\langle r| \otimes \hat{\mathcal{I}}_2 \otimes |r\rangle_c\langle r|, \quad (6)$$

where $\hat{H}_{12}$ is given in Eq. (1), and $\hat{H}_c = \Omega_c(t)|0\rangle_c\langle r|/2 + \mathrm{H.c.}$ with $\Omega_c(t) = \Omega_{cm}\cos(\omega_c t)$ modulated in amplitude. On the basis of the SWAP gate, the Hamiltonian Eq. (6) is reduced to

$$\hat{H}'_{12c} = \hat{H}_e \otimes \hat{\mathcal{I}}_c + \hat{\mathcal{I}}_1 \otimes \hat{\mathcal{I}}_2 \otimes \hat{H}_c + (V_{1c} + V_{2c})|rrr\rangle\langle rrr|, \quad (7)$$

where $\hat{H}_e$ is given in Eq. (3). The diagram of this Hamiltonian is visualized in Fig. 1(b). Furthermore, this three-atom dynamics can be simplified toward the form (see Appendix C)

$$\hat{H}_{\mathrm{eff}} = \hat{H}_e \otimes |1\rangle_c\langle 1|, \quad (8)$$

when considering the condition $|\omega_c| \gg |\Omega_{cm}|/4$ and $|\Omega_{cm}/4 \pm \delta'| \gg |\Omega_e|/\sqrt{2}$ as well as the relation $V_{1c} + V_{2c} = \omega_c - \Delta_{rrr}$ with $\Delta_{rrr} = \Omega_e^2/2\omega_c + \Omega_{cm}^2/32\omega_c$ being a small Stark shift of the triply excited Rydberg state $|rrr\rangle$. Equation (8) indicates that when and only when the state of the control atom is $|1\rangle$, the SWAP gate on atoms 1 and 2 works, which is exactly a CSWAP gate $U_{\mathrm{CSWAP}} = \hat{\mathcal{I}}_1 \otimes \hat{\mathcal{I}}_2 \otimes |0\rangle_c\langle 0| + U_{\mathrm{SWAP}} \otimes |1\rangle_c\langle 1|$. Besides, according to different assignments of δ' in $\hat{H}_e$, the CSWAP gate can be implemented based on not only the resonant RAB but also on the modified RAB with enhanced robustness, similar to the

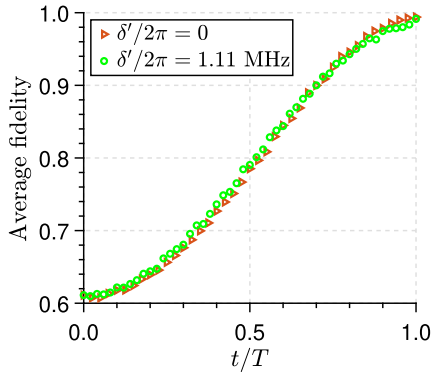

Fig. 5. Time-dependent average fidelities of the CSWAP gate with $\{\delta' = 0, T = 3.87\ \mu s\}$ and $\{\delta'/2\pi = 1.11$ MHz, $T = 33.28\ \mu s\}$, respectively. Atomic decay is not considered. $\Omega_{cm}/2\pi = 12$ MHz and $\omega_c/2\pi = 142$ MHz, and $V_{1c}/2\pi = V_{2c}/2\pi = 70.98$ MHz.

implementation of the SWAP gate. In Fig. 5, we numerically calculate the average fidelity of the CSWAP gate achieved by the resonant RAB ($\delta' = 0$) and the modified RAB ($\delta'/2\pi = 1.11$ MHz), and two lines both reach high average fidelities >0.991, which is over the error-correction threshold in a surface code scheme [70].

From Eq. (8), we know that the triply excited Rydberg state $|rrr\rangle_{12c}$ is not involved in the CSWAP gate procedure. Besides, the modified condition $|\delta'| \gg |\Omega_e|/2$ of RAB suppresses the excitation of the doubly excited Rydberg state $|rr\rangle_{12}$. For more detailed illustration, in Fig. 6 we calculate numerical Rydberg excitation probabilities with different excitation numbers for

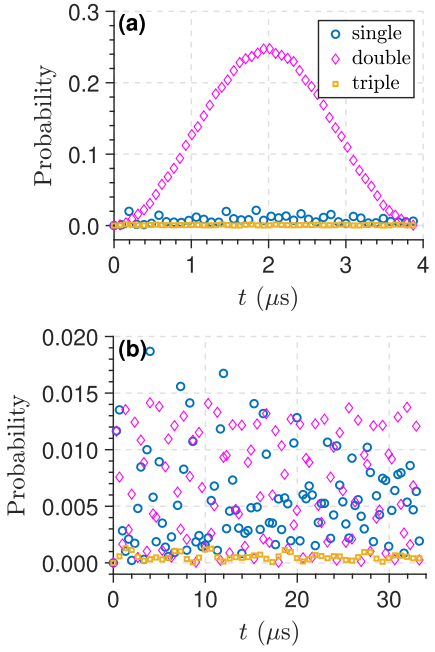

Fig. 6. Rydberg excitation probabilities during the CSWAP gate procedure with different excitation numbers for (a) the resonant RAB with $\delta' = 0$ and (b) the modified RAB with $\delta'/2\pi = 1.11$ MHz, respectively. Three-atom initial product state $|\Psi_0\rangle = (|0\rangle_1 - |1\rangle_1)/\sqrt{2} \otimes (|0\rangle_2 - |1\rangle_2)/\sqrt{2} \otimes (|0\rangle_c - |1\rangle_c)/\sqrt{2}$ is specified.

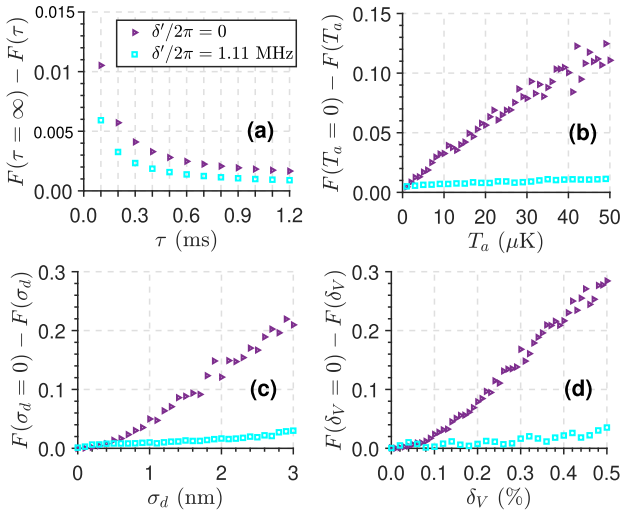

Fig. 7. Infidelities of the CSWAP gates caused by (a) atomic decay with different lifetimes of the Rydberg state, (b) motional dephasing with different atomic temperatures, (c) standard deviations of the distance between the two target atoms, and (d) deviations in the RRI strength between the two target atoms. Each point in (b), (c), and (d) denotes the average of 201 results.

cases of the resonant RAB and the modified RAB. From Fig. 6, we learn that the triply excited state $|rrr\rangle_{12c}$ is suppressed for both cases. Besides, similar to the SWAP gates, the single-excitation states are also hardly populated for both cases, and the double-excitation state $|rr\rangle_{12}$ is also constrained for the modified RAB, whose excitation probability is always below 0.015.

The CSWAP gate is on the basis of the SWAP gate, so the gate performance is similar to the SWAP gate, including gate time and robustness. Because Rydberg excitation of any one of the three atoms can be avoided for the modified RAB [see Fig. 6(b)], the infidelity caused by atomic decay from Rydberg states into ground states will be negligible. The effect on the CSWAP gate fidelity of motional dephasing that occurs during Rydberg excitation is also slight because only virtual excitation for the three atoms attends throughout the gate procedure. In addition, the infidelity in the case of the modified RAB, caused by moderate fluctuations of distances among the three atoms, will be much less than that in the conventional RAB-based quantum gates. These properties are identified in Fig. 7.

5. CONCLUSION

To conclude, we have proposed effective schemes to implement one-step Rydberg-mediated SWAP and CSWAP gates on neutral atomic systems under a Rydberg antiblockade regime. The use of resonant amplitude-modulated fields enables a Λ-type Rydberg antiblockade structure, which facilitates a Raman-like process connecting two odd-parity computational states of two atoms and thus the implementation of the SWAP gate. Besides, the robustness of gates is enhanced through modifying the condition of the Rydberg antiblockade. The introduction of a periodically driven control atom makes the execution of the SWAP gate depend on the state of the control atom, so a CSWAP gate

is achieved with the same gate time and similar gate performance to the SWAP gate. Our work fills the gap of directly implementing one-step Rydberg-mediated SWAP and CSWAP gates and circumvents common issues in Rydberg antiblockade based gates.

APPENDIX A: DERIVATION OF EQ. (3)

With the two-atom basis $\{|jk\rangle\}$ $(j,k=0,1,r)$, the full Hamiltonian of two atoms is

$$\begin{aligned}\hat{H}_0=&\frac{1}{2}[\Omega_{0m}\cos(\omega_0 t)(|00\rangle\langle r0|+|01\rangle\langle r1|+|0r\rangle\langle rr|+|00\rangle\langle 0r|\\&+|10\rangle\langle 1r|+|r0\rangle\langle rr|)+\Omega_{1m}\cos(\omega_1 t)(|10\rangle\langle r0|+|11\rangle\langle r1|\\&+|1r\rangle\langle rr|+|01\rangle\langle 0r|+|11\rangle\langle 1r|+|r1\rangle\langle rr|)+\text{H.c.}]\\&+V|rr\rangle\langle rr|. \qquad \textbf{(A1)}\end{aligned}$$

We transform Eq. (A1) into the frame defined by $\hat{U}_0=\exp(it\delta|rr\rangle\langle rr|)$ with $\delta=V-\delta_0=\omega_1-\omega_0\gg\delta_0$ and obtain $\hat{H}_1=\hat{U}_0(\hat{H}_0-i\frac{\partial}{\partial t})\hat{U}_0^{\dagger}=\hat{H}_1'+\delta_0|rr\rangle\langle rr|$ with

$$\begin{aligned}\hat{H}_1'=&\frac{\Omega_{0m}}{4}\{(e^{i\omega_0 t}+e^{-i\omega_0 t})(|00\rangle\langle r0|+|01\rangle\langle r1|+|00\rangle\langle 0r|\\&+|10\rangle\langle 1r|)+[e^{i(\omega_0-\delta)t}+e^{-i\omega_1 t}](|0r\rangle\langle rr|+|r0\rangle\langle rr|)\}\\&+\frac{\Omega_{1m}}{4}\{(e^{i\omega_1 t}+e^{-i\omega_1 t})(|10\rangle\langle r0|+|11\rangle\langle r1|+|01\rangle\langle 0r|\\&+|11\rangle\langle 1r|)+[e^{i\omega_0 t}+e^{-i(\omega_1+\delta)t}](|1r\rangle\langle rr|+|r1\rangle\langle rr|)\}\\&+\text{H.c.} \qquad \textbf{(A2)}\end{aligned}$$

When considering $|\omega_0|,|\omega_1|,|\omega_0-\delta|,|\omega_1+\delta|\gg|\Omega_{0m}|/4$, $|\Omega_{1m}|/4$, the terms

$$\begin{aligned}&\frac{\Omega_{0m}}{4}(e^{i\omega_0 t}+e^{-i\omega_0 t})(|00\rangle\langle r0|+|00\rangle\langle 0r|)\\&+\frac{\Omega_{1m}}{4}(e^{i\omega_1 t}+e^{-i\omega_1 t})(|11\rangle\langle r1|+|11\rangle\langle 1r|)+\text{H.c.}\end{aligned}$$

can be neglected under the rotating-wave approximation because the transitions are of large detunings; besides, the involved even-parity states, $|00\rangle$ and $|11\rangle$, cannot be effectively coupled resonantly to other states yet through two-photon processes. In addition, under the second-order perturbation theory, the even-parity computational states $|00\rangle$ and $|11\rangle$ have a zero-value sum of Stark shifts, and all single-excitation states are uncoupled to the four computational states. Then, the remaining part of Eq. (A2) can be sorted as

$$\begin{aligned}\hat{H}_1'\simeq&\left[\frac{\Omega_{0m}}{4}(e^{i\omega_0 t}+e^{-i\omega_0 t})|01\rangle\langle r1|+\frac{\Omega_{1m}}{4}e^{i\omega_0 t}|r1\rangle\langle rr|\right]\\&+\left[\frac{\Omega_{1m}}{4}(e^{i\omega_1 t}+e^{-i\omega_1 t})|01\rangle\langle 0r|+\frac{\Omega_{0m}}{4}e^{-i\omega_1 t}|0r\rangle\langle rr|\right]\\&+\left[\frac{\Omega_{0m}}{4}(e^{i\omega_0 t}+e^{-i\omega_0 t})|10\rangle\langle 1r|+\frac{\Omega_{1m}}{4}e^{i\omega_0 t}|1r\rangle\langle rr|\right]\\&+\left[\frac{\Omega_{1m}}{4}(e^{i\omega_1 t}+e^{-i\omega_1 t})|10\rangle\langle r0|+\frac{\Omega_{0m}}{4}e^{-i\omega_0 t}|r0\rangle\langle rr|\right]\\&+\frac{\Omega_{0m}}{4}e^{i(\omega_0-\delta)t}(|0r\rangle\langle rr|+|r0\rangle\langle rr|)\\&+\frac{\Omega_{1m}}{4}e^{-i(\omega_1+\delta)t}(|1r\rangle\langle rr|+|r1\rangle\langle rr|)+\text{H.c.} \qquad \textbf{(A3)}\end{aligned}$$

With the second-order perturbation theory, the first four terms in Eq. (A3) induce the effective coupling of $|01\rangle\leftrightarrow|rr\rangle\leftrightarrow|10\rangle$ and Stark shifts of $|rr\rangle$, while the last two terms induce solely Stark shifts of $|rr\rangle$. Therefore, a final effective Hamiltonian of the two atoms can be obtained as

$$\hat{H}_e=\left[\frac{\Omega_e}{2}(|01\rangle\langle rr|+|10\rangle\langle rr|)+\text{H.c.}\right]+\delta'|rr\rangle\langle rr|, \qquad \textbf{(A4)}$$

in which $\Omega_e=\Omega_{0m}\Omega_{1m}/8\omega_1-\Omega_{0m}\Omega_{1m}/8\omega_0$ and $\delta'=\Delta_{rr}+\delta_0$ with $\Delta_{rr}=\Omega_{0m}^2/8\omega_1-\Omega_{1m}^2/8\omega_0+\Omega_{1m}^2/8(\omega_1+\delta)-\Omega_{0m}^2/8(\omega_0-\delta)$ being the sum Stark shift of $|rr\rangle$.

APPENDIX B: DEFINITION OF THE TRACE-PRESERVING-QUANTUM-OPERATOR-BASED AVERAGE FIDELITY

According to Nielsen's work [63], the trace-preserving-quantum-operator-based average fidelity of a quantum gate is defined as

$$\bar{F}(\varepsilon,\hat{U})=\left\{\sum_{j=1}^{4^N}\text{tr}[\hat{U}\hat{u}_j^{\dagger}\hat{U}^{\dagger}\varepsilon(\hat{u}_j)]+l^2\right\}\Big/l^2(l+1), \qquad \textbf{(B1)}$$

where $\hat{U}$ is the ideal gate, $\hat{u}_j=\otimes_k^N\hat{\sigma}_k$ is the tensor of Pauli matrices $\hat{\sigma}_k\in\{\hat{I},\hat{\sigma}^x,\hat{\sigma}^y,\hat{\sigma}^z\}$ on computational states $\{|0\rangle,|1\rangle\}$, and $l=2^N$ for an N-qubit gate. $\varepsilon(\hat{u}_j)$ is a trace-preserving quantum operation obtained through our logic gates that can be solved by the master equation.

APPENDIX C: DERIVATION OF EQ. (8)

First, it is clear that the evolution from three-atom computational states $|001\rangle_{12c}$ and $|111\rangle_{12c}$ is prohibited. For $|000\rangle_{12c}$ or $|110\rangle_{12c}$, the governing Hamiltonian is $\hat{H}_{\beta 0}=\Omega_{cm}(e^{i\omega_c t}+e^{-i\omega_c t})|\beta 0\rangle_{12c}\langle\beta r|/4+\text{H.c.}$ $(\beta=00,11)$. No evolution will occur when $|\omega_c|\gg|\Omega_{cm}|/4$ is considered, because the laser-induced transitions are largely detuned, and the sum Stark shift of $|\beta 0\rangle_{12c}$ is zero.

When the state of three atoms is $|010\rangle_{12c}$ or $|100\rangle_{12c}$, the governing Hamiltonian of the three atoms is $\hat{H}_2=\hat{H}_2'+\delta'|rr\rangle_{12}\langle rr|+(V_{1c}+V_{2c})|rrr\rangle_{12c}\langle rrr|$ with

$$\begin{aligned}\hat{H}_2'=&\frac{\Omega_{cm}}{4}(e^{i\omega_c t}+e^{-i\omega_c t})(|010\rangle_{12c}\langle 01r|+|100\rangle_{12c}\langle 10r|\\&+|rr0\rangle_{12c}\langle rrr|)+\frac{\Omega_e}{2}(|010\rangle_{12c}\langle rr0|+|100\rangle_{12c}\langle rr0|\\&+|01r\rangle_{12c}\langle rrr|+|10r\rangle_{12c}\langle rrr|)+\text{H.c.} \qquad \textbf{(C1)}\end{aligned}$$

Transforming $\hat{H}_2$ to the frame defined by $\hat{U}_1=\exp(it\omega_c|rrr\rangle_{12c}\langle rrr|)$, one can obtain $\hat{H}_3=\hat{H}_3'+\delta'|rr\rangle_{12}\langle rr|+(V_{1c}+V_{2c}-\omega_c)|rrr\rangle_{12c}\langle rrr|$ with

$$\begin{aligned}\hat{H}_3'=&\frac{\Omega_{cm}}{4}[(e^{i\omega_c t}+e^{-i\omega_c t})(|010\rangle_{12c}\langle 01r|+|100\rangle_{12c}\langle 10r|)\\&+(1+e^{-2i\omega_c t})|rr0\rangle_{12c}\langle rrr|]+\frac{\Omega_e}{2}(|010\rangle_{12c}\langle rr0|\\&+|100\rangle_{12c}\langle rr0|+|01r\rangle_{12c}\langle rrr|e^{-i\omega_c t}+|10r\rangle_{12c}\langle rrr|e^{-i\omega_c t})\\&+\text{H.c.} \qquad \textbf{(C2)}\end{aligned}$$

Through neglecting frequent oscillations under rotating-wave approximation with the condition $|\omega_c|\gg|\Omega_{cm}|/4,|\Omega_e|/2$, $\hat{H}_3'$ becomes

$$\hat{H}_3'' = \left[\frac{\Omega_{cm}}{4}|rr0\rangle_{12c}\langle rrr| + \frac{\Omega_e}{2}(|010\rangle_{12c}\langle rr0| + |100\rangle_{12c}\langle rr0|) + \text{H.c.}\right] + \Delta_{rrr}|rrr\rangle_{12c}\langle rrr|, \quad \text{(C3)}$$

with $\Delta_{rrr} = \Omega_e^2/2\omega_c + \Omega_{cm}^2/32\omega_c$ being the Stark shift of $|rrr\rangle_{12c}$. In this case, an effective three-atom Hamiltonian of $\hat{H}_3$ can be obtained as $\hat{H}_4 = \hat{H}_3'' + \delta'|rr\rangle_{12}\langle rr|$ with the condition $V_{1c} + V_{2c} = \omega_c - \Delta_{rrr}$. $\hat{H}_4$ can be rewritten as

$$\hat{H}_4 = \left[\frac{\Omega_e}{\sqrt{2}}(|010\rangle_{12c} + |100\rangle_{12c})(\langle\phi_0| + \langle\phi_1|) + \text{H.c.}\right] + \frac{\Omega_{cm}}{4}\sum_{n=0}^{1}(-1)^n|\phi_n\rangle\langle\phi_n| + \delta'|rr\rangle_{12}\langle rr|, \quad \text{(C4)}$$

in which $|\phi_n\rangle = (|rr0\rangle_{12c} + (-1)^n|rrr\rangle_{12c})/\sqrt{2}$. Transforming $\hat{H}_4$ to the frame defined by $\hat{U}_2 = \exp(it\hat{A})$ with $\hat{A} = \Omega_{cm}\sum_{n=0}^{1}(-1)^n|\phi_n\rangle\langle\phi_n|/4 + \delta'|rr\rangle_{12}\langle rr|$, one can obtain a Hamiltonian with entirely off-resonant interactions

$$\hat{H}_5 = \frac{\Omega_e}{\sqrt{2}}(|010\rangle_{12c} + |100\rangle_{12c})[\langle\phi_0|e^{-it(\Omega_{cm}/4+\delta')} + \langle\phi_1|e^{it(\Omega_{cm}/4-\delta')}] + \text{H.c.} \quad \text{(C5)}$$

When the condition $|\Omega_{cm}/4 \pm \delta'| \gg |\Omega_e|/\sqrt{2}$ is satisfied, transitions from $|010\rangle_{12c}$ or $|100\rangle_{12c}$ can be banned.

Now that the evolution from six three-atom computational states, including $|000\rangle_{12c}$, $|010\rangle_{12c}$, $|100\rangle_{12c}$, $|110\rangle_{12c}$, $|001\rangle_{12c}$, and $|111\rangle_{12c}$, is banned, the dynamics of the three atoms can be governed by an effective Hamiltonian

$$\hat{H}_{\text{eff}} = \left[\frac{\Omega_e}{2}(|011\rangle_{12c} + |101\rangle_{12c})\langle rr1| + \text{H.c.}\right] + \delta'|rr1\rangle_{12c}\langle rr1|, \quad \text{(C6)}$$

which is exactly Eq. (8) in the main text.

Funding. National Natural Science Foundation of China (NSFC) (11675046, 21973023, 11804308); Program for Innovation Research of Science in Harbin Institute of Technology (A201412); Postdoctoral Scientific Research Developmental Fund of Heilongjiang Province (LBH-Q15060); Natural Science Foundation of Henan Province (202300410481).

Disclosures. The authors declare no conflicts of interest.

REFERENCES

1. M. Saffman, T. G. Walker, and K. Mølmer, "Quantum information with Rydberg atoms," Rev. Mod. Phys. **82**, 2313–2363 (2010).
2. M. Saffman, "Quantum computing with atomic qubits and Rydberg interactions: progress and challenges," J. Phys. B **49**, 202001 (2016).
3. A. Browaeys and T. Lahaye, "Many-body physics with individually controlled Rydberg atoms," Nat. Phys. **16**, 132–142 (2020).
4. Z.-Y. Zhang, T.-Y. Zhang, Z.-K. Liu, D.-S. Ding, and B.-S. Shi, "Research progress of Rydberg many-body interaction," Acta Phys. Sin. **69**, 080301 (2020).
5. H. Levine, A. Keesling, A. Omran, H. Bernien, S. Schwartz, A. S. Zibrov, M. Endres, M. Greiner, V. Vuletić, and M. D. Lukin, "High-fidelity control and entanglement of Rydberg-atom qubits," Phys. Rev. Lett. **121**, 123603 (2018).
6. T. M. Graham, M. Kwon, B. Grinkemeyer, Z. Marra, X. Jiang, M. T. Lichtman, Y. Sun, M. Ebert, and M. Saffman, "Rydberg-mediated entanglement in a two-dimensional neutral atom qubit array," Phys. Rev. Lett. **123**, 230501 (2019).
7. H. Levine, A. Keesling, G. Semeghini, A. Omran, T. T. Wang, S. Ebadi, H. Bernien, M. Greiner, V. Vuletić, H. Pichler, and M. D. Lukin, "Parallel implementation of high-fidelity multiqubit gates with neutral atoms," Phys. Rev. Lett. **123**, 170503 (2019).
8. P. Schauß, , J. Zeiher, T. Fukuhara, S. Hild, M. Cheneau, T. Macr, T. Pohl, I. Bloch, and C. Gross, "Crystallization in Ising quantum magnets," Science **347**, 1455–1458 (2015).
9. H. Labuhn, D. Barredo, S. Ravets, S. de Léséleuc, T. Macrì, T. Lahaye, and A. Browaeys, "Tunable two-dimensional arrays of single Rydberg atoms for realizing quantum Ising models," Nature **534**, 667–670 (2016).
10. H. Bernien, S. Schwartz, A. Keesling, H. Levine, A. Omran, H. Pichler, S. Choi, A. S. Zibrov, M. Endres, M. Greiner, V. Vuletić, and M. D. Lukin, "Probing many-body dynamics on a 51-atom quantum simulator," Nature **551**, 579–584 (2017).
11. A. Omran, H. Levine, A. Keesling, G. Semeghini, T. T. Wang, S. Ebadi, H. Bernien, A. S. Zibrov, H. Pichler, S. Choi, J. Cui, M. Rossignolo, P. Rembold, S. Montangero, T. Calarco, M. Endres, M. Greiner, V. Vuletić, and M. D. Lukin, "Generation and manipulation of Schrödinger cat states in Rydberg atom arrays," Science **365**, 570–574 (2019).
12. I. S. Madjarov, J. P. Covey, A. L. Shaw, J. Choi, A. Kale, A. Cooper, H. Pichler, V. Schkolnik, J. R. Williams, and M. Endres, "High-fidelity entanglement and detection of alkaline-earth Rydberg atoms," Nat. Phys. **16**, 857–861 (2020).
13. D. Jaksch, J. I. Cirac, P. Zoller, S. L. Rolston, R. Côté, and M. D. Lukin, "Fast quantum gates for neutral atoms," Phys. Rev. Lett. **85**, 2208–2211 (2000).
14. M. D. Lukin, M. Fleischhauer, R. Cote, L. M. Duan, D. Jaksch, J. I. Cirac, and P. Zoller, "Dipole blockade and quantum information processing in mesoscopic atomic ensembles," Phys. Rev. Lett. **87**, 037901 (2001).
15. E. Urban, T. A. Johnson, T. Henage, L. Isenhower, D. D. Yavuz, T. G. Walker, and M. Saffman, "Observation of Rydberg blockade between two atoms," Nat. Phys. **5**, 110–114 (2009).
16. A. Gaëtan, Y. Miroshnychenko, T. Wilk, A. Chotia, M. Viteau, D. Comparat, P. Pillet, A. Browaeys, and P. Grangier, "Observation of collective excitation of two individual atoms in the Rydberg blockade regime," Nat. Phys. **5**, 115–118 (2009).
17. X.-F. Shi, "Deutsch, Toffoli, and CNOT gates via Rydberg blockade of neutral atoms," Phys. Rev. Appl. **9**, 051001 (2018).
18. C.-P. Shen, J.-L. Wu, S.-L. Su, and E. Liang, "Construction of robust Rydberg controlled-phase gates," Opt. Lett. **44**, 2036–2039 (2019).
19. K.-Y. Liao, X.-H. Liu, Z. Li, and Y.-X. Du, "Geometric Rydberg quantum gate with shortcuts to adiabaticity," Opt. Lett. **44**, 4801–4804 (2019).
20. B.-J. Liu, S.-L. Su, and M.-H. Yung, "Nonadiabatic noncyclic geometric quantum computation in Rydberg atoms," Phys. Rev. Res. **2**, 043130 (2020).
21. K. Bergmann, H. Theuer, and B. W. Shore, "Coherent population transfer among quantum states of atoms and molecules," Rev. Mod. Phys. **70**, 1003–1025 (1998).
22. N. V. Vitanov, A. A. Rangelov, B. W. Shore, and K. Bergmann, "Stimulated Raman adiabatic passage in physics, chemistry, and beyond," Rev. Mod. Phys. **89**, 015006 (2017).
23. D. Petrosyan, F. Motzoi, M. Saffman, and K. Mølmer, "High-fidelity Rydberg quantum gate via a two-atom dark state," Phys. Rev. A **96**, 042306 (2017).
24. I. I. Beterov, G. N. Hamzina, E. A. Yakshina, D. B. Tretyakov, V. M. Entin, and I. I. Ryabtsev, "Adiabatic passage of radio-frequency-assisted Förster resonances in Rydberg atoms for two-qubit gates and the generation of bell states," Phys. Rev. A **97**, 032701 (2018).
25. M. Khazali and K. Mølmer, "Fast multiqubit gates by adiabatic evolution in interacting excited-state manifolds of Rydberg atoms and superconducting circuits," Phys. Rev. X **10**, 021054 (2020).

26. M. Saffman, I. I. Beterov, A. Dalal, E. J. Páez, and B. C. Sanders, "Symmetric Rydberg controlled-Z gates with adiabatic pulses," Phys. Rev. A **101**, 062309 (2020).
27. A. Mitra, M. J. Martin, G. W. Biedermann, A. M. Marino, P. M. Poggi, and I. H. Deutsch, "Robust Mølmer-Sørensen gate for neutral atoms using rapid adiabatic Rydberg dressing," Phys. Rev. A **101**, 030301 (2020).
28. C. Ates, T. Pohl, T. Pattard, and J. M. Rost, "Antiblockade in Rydberg excitation of an ultracold lattice gas," Phys. Rev. Lett. **98**, 023002 (2007).
29. T. Pohl and P. R. Berman, "Breaking the dipole blockade: nearly resonant dipole interactions in few-atom systems," Phys. Rev. Lett. **102**, 013004 (2009).
30. J. Qian, Y. Qian, M. Ke, X.-L. Feng, C. H. Oh, and Y. Wang, "Breakdown of the dipole blockade with a zero-area phase-jump pulse," Phys. Rev. A **80**, 053413 (2009).
31. T. Amthor, C. Giese, C. S. Hofmann, and M. Weidemüller, "Evidence of antiblockade in an ultracold Rydberg gas," Phys. Rev. Lett. **104**, 013001 (2010).
32. W. Li, C. Ates, and I. Lesanovsky, "Nonadiabatic motional effects and dissipative blockade for Rydberg atoms excited from optical lattices or microtraps," Phys. Rev. Lett. **110**, 213005 (2013).
33. S. Basak, Y. Chougale, and R. Nath, "Periodically driven array of single Rydberg atoms," Phys. Rev. Lett. **120**, 123204 (2018).
34. S.-L. Su, E. Liang, S. Zhang, J.-J. Wen, L.-L. Sun, Z. Jin, and A.-D. Zhu, "One-step implementation of the Rydberg-Rydberg-interaction gate," Phys. Rev. A **93**, 012306 (2016).
35. S. L. Su, H. Z. Shen, E. Liang, and S. Zhang, "One-step construction of the multiple-qubit Rydberg controlled-phase gate," Phys. Rev. A **98**, 032306 (2018).
36. J.-L. Wu, S.-L. Su, Y. Wang, J. Song, Y. Xia, and Y. Jiang, "Effective Rabi dynamics of Rydberg atoms and robust high-fidelity quantum gates with a resonant amplitude-modulation field," Opt. Lett. **45**, 1200–1203 (2020).
37. T. H. Xing, X. Wu, and G. F. Xu, "Nonadiabatic holonomic three-qubit controlled gates realized by one-shot implementation," Phys. Rev. A **101**, 012306 (2020).
38. H.-D. Yin, X.-X. Li, G.-C. Wang, and X.-Q. Shao, "One-step implementation of Toffoli gate for neutral atoms based on unconventional Rydberg pumping," Opt. Express **28**, 35576–35587 (2020).
39. J.-L. Wu, J. Song, and S.-L. Su, "Resonant-interaction-induced Rydberg antiblockade and its applications," Phys. Lett. A **384**, 126039 (2020).
40. S.-L. Su, F.-Q. Guo, J.-L. Wu, Z. Jin, X. Q. Shao, and S. Zhang, "Rydberg antiblockade regimes: dynamics and applications," Europhys. Lett. **131**, 53001 (2020).
41. M. Saffman, X. L. Zhang, A. T. Gill, L. Isenhower, and T. G. Walker, "Rydberg state mediated quantum gates and entanglement of pairs of neutral atoms," J. Phys. Conf. Ser. **264**, 012023 (2011).
42. S. de Léséleuc, D. Barredo, V. Lienhard, A. Browaeys, and T. Lahaye, "Analysis of imperfections in the coherent optical excitation of single atoms to Rydberg states," Phys. Rev. A **97**, 053803 (2018).
43. E. Fredkin and T. Toffoli, "Conservative logic," Int. J. Theor. Phys. **21**, 219–253 (1983).
44. N. Schuch and J. Siewert, "Natural two-qubit gate for quantum computation using the XY interaction," Phys. Rev. A **67**, 032301 (2003).
45. L. Isenhower, M. Saffman, and K. Mølmer, "Multibit C_kNOT quantum gates via Rydberg blockade," Quantum Inf. Process. **10**, 755 (2011).
46. R. J. Spiteri, M. Schmidt, J. Ghosh, E. Zahedinejad, and B. C. Sanders, "Quantum control for high-fidelity multi-qubit gates," New J. Phys. **20**, 113009 (2018).
47. W. Feng and D.-W. Wang, "Quantum Fredkin gate based on synthetic three-body interactions in superconducting circuits," Phys. Rev. A **101**, 062312 (2020).
48. S. E. Rasmussen, K. Groenland, R. Gerritsma, K. Schoutens, and N. T. Zinner, "Single-step implementation of high-fidelity *n*-bit Toffoli gates," Phys. Rev. A **101**, 022308 (2020).
49. R. Barends, C. M. Quintana, A. G. Petukhov, Y. Chen, D. Kafri, K. Kechedzhi, R. Collins, O. Naaman, S. Boixo, F. Arute, K. Arya, D. Buell, B. Burkett, Z. Chen, B. Chiaro, A. Dunsworth, B. Foxen, A. Fowler, C. Gidney, M. Giustina, R. Graff, T. Huang, E. Jeffrey, J. Kelly, P. V. Klimov, F. Kostritsa, D. Landhuis, E. Lucero, M. McEwen, A. Megrant, X. Mi, J. Mutus, M. Neeley, C. Neill, E. Ostby, P. Roushan, D. Sank, K. J. Satzinger, A. Vainsencher, T. White, J. Yao, P. Yeh, A. Zalcman, H. Neven, V. N. Smelyanskiy, and J. M. Martinis, "Diabatic gates for frequency-tunable superconducting qubits," Phys. Rev. Lett. **123**, 210501 (2019).
50. W. Ning, X.-J. Huang, P.-R. Han, H. Li, H. Deng, Z.-B. Yang, Z.-R. Zhong, Y. Xia, K. Xu, D. Zheng, and S.-B. Zheng, "Deterministic entanglement swapping in a superconducting circuit," Phys. Rev. Lett. **123**, 060502 (2019).
51. N. Sangouard, C. Simon, H. de Riedmatten, and N. Gisin, "Quantum repeaters based on atomic ensembles and linear optics," Rev. Mod. Phys. **83**, 33–80 (2011).
52. I. L. Chuang and Y. Yamamoto, "Quantum bit regeneration," Phys. Rev. Lett. **76**, 4281–4284 (1996).
53. H. Buhrman, R. Cleve, J. Watrous, and R. de Wolf, "Quantum fingerprinting," Phys. Rev. Lett. **87**, 167902 (2001).
54. B. K. Behera, T. Reza, A. Gupta, and P. K. Panigrahi, "Designing quantum router in IBM quantum computer," Quantum Inf. Process. **18**, 328 (2019).
55. H.-Z. Wu, Z.-B. Yang, and S.-B. Zheng, "Quantum state swap for two trapped Rydberg atoms," Chin. Phys. B **21**, 040305 (2012).
56. X.-F. Shi, F. Bariani, and T. A. B. Kennedy, "Entanglement of neutral-atom chains by spin-exchange Rydberg interaction," Phys. Rev. A **90**, 062327 (2014).
57. A. W. Glaetzle, M. Dalmonte, R. Nath, C. Gross, I. Bloch, and P. Zoller, "Designing frustrated quantum magnets with laser-dressed Rydberg atoms," Phys. Rev. Lett. **114**, 173002 (2015).
58. M. Gärttner, K. P. Heeg, T. Gasenzer, and J. Evers, "Dynamic formation of Rydberg aggregates at off-resonant excitation," Phys. Rev. A **88**, 043410 (2013).
59. S.-L. Su, Y. Gao, E. Liang, and S. Zhang, "Fast Rydberg antiblockade regime and its applications in quantum logic gates," Phys. Rev. A **95**, 022319 (2017).
60. X.-Y. Zhu, E. Liang, and S.-L. Su, "Rydberg-atom-based controlled arbitrary-phase gate and its applications," J. Opt. Soc. Am. B **36**, 1937–1944 (2019).
61. D. James and J. Jerke, "Effective Hamiltonian theory and its applications in quantum information," Can. J. Phys. **85**, 625–632 (2007).
62. W. Shao, C. Wu, and X.-L. Feng, "Generalized James' effective Hamiltonian method," Phys. Rev. A **95**, 032124 (2017).
63. M. A. Nielsen, "A simple formula for the average gate fidelity of a quantum dynamical operation," Phys. Lett. A **303**, 249–252 (2002).
64. C.-Y. Guo, L.-L. Yan, S. Zhang, S.-L. Su, and W. Li, "Optimized geometric quantum computation with a mesoscopic ensemble of Rydberg atoms," Phys. Rev. A **102**, 042607 (2020).
65. F.-Q. Guo, J.-L. Wu, X.-Y. Zhu, Z. Jin, Y. Zeng, S. Zhang, L.-L. Yan, M. Feng, and S.-L. Su, "Complete and nondestructive distinguishment of many-body Rydberg entanglement via robust geometric quantum operations," Phys. Rev. A **102**, 062410 (2020).
66. E. Brion, L. H. Pedersen, and K. Mølmer, "Implementing a neutral atom Rydberg gate without populating the Rydberg state," J. Phys. B **40**, S159–S166 (2007).
67. J.-L. Wu, Y. Wang, J.-X. Han, S.-L. Su, Y. Xia, Y. Jiang, and J. Song, "Resilient quantum gates on periodically driven Rydberg atoms," Phys. Rev. A **103**, 012601 (2021).
68. X.-F. Shi, "Fast, accurate, and realizable two-qubit entangling gates by quantum interference in detuned Rabi cycles of Rydberg atoms," Phys. Rev. Appl. **11**, 044035 (2019).
69. X.-F. Shi, "Suppressing motional dephasing of ground-Rydberg transition for high-fidelity quantum control with neutral atoms," Phys. Rev. Appl. **13**, 024008 (2020).
70. A. G. Fowler, A. M. Stephens, and P. Groszkowski, "High-threshold universal quantum computation on the surface code," Phys. Rev. A **80**, 052312 (2009).